

Charming top interactions with a neutral Higgs Boson decaying into $\tau^+\tau^-$ at the LHC

Chenyu Fang*, Phillip Gutierrez† and Chung Kao‡

*Homer L. Dodge Department of Physics and Astronomy,
University of Oklahoma, Norman, OK 73019, USA*

(Dated: November 12, 2025)

Abstract

We investigate the discovery potential of flavor changing neutral Higgs (FCNH) interactions in top quark decays at the LHC. A general two Higgs doublet model (2HDM) is adopted to study the top quark decay $t \rightarrow c\phi^0$, where ϕ^0 is either a CP-even heavy neutral scalar (H^0), or a CP-odd pseudoscalar (A^0), followed by the Higgs boson decaying into $\tau^+\tau^-$. The complete process is $pp \rightarrow t\bar{t} \rightarrow tc\phi^0 \rightarrow (bjj)(c\tau_{lep}\tau_{had}) + X$, where t or \bar{t} become virtual when $m_\phi > m_t - m_c$, τ_{lep} and τ_{had} represent the τ leptonic decay ($\tau^\pm \rightarrow \ell^\pm + \cancel{E}_T$) and the τ hadronic decay ($\tau^\pm \rightarrow j_\tau + \cancel{E}_T$), respectively. We evaluate the cross section applying realistic selection criteria for the FCNH signal and the dominant physics background at the parton-level. In addition, we employ MADGRAPH, PYTHIA 8, and DELPHES to perform a realistic event-level Monte Carlo simulation analysis. The collinear approximation is applied since the τ 's from Higgs boson decays are highly boosted such that τ_{lep} and τ_{had} momenta are approximately in the same direction as the τ 's, which enables the reconstruction of the Higgs boson mass. The energy of the charm quark provides an additional kinematic variable that discriminates the signal from the background. The measured properties of the 125 GeV Higgs boson at the LHC implies the alignment limit for 2HDMs ($\lambda_{tch} \propto \cos(\beta-\alpha) \approx 0$). This means the FCNH couplings for the heavy Higgs bosons (H^0 and A^0) will not be suppressed [$\lambda_{tch} \propto \sin(\beta-\alpha) \approx 1$]. We study the discovery potential for the heavy neutral Higgs bosons at the LHC with collider energies of $\sqrt{s} = 13$ TeV, 13.6 TeV and 14 TeV, and find the High-Luminosity LHC offers great promise for the discovery of heavier Higgs bosons from $t \rightarrow c\phi^0$ or $t^* \rightarrow c\phi^0$.

PACS numbers:

* E-mail address: chenyu.fang@ou.edu

† E-mail address: pgutierrez@ou.edu

‡ E-mail address: Chung.Kao@ou.edu

I. INTRODUCTION

The discovery of a 125 GeV CP-even scalar Higgs boson (h^0) in 2012 [1, 2] completed the particle content of the Standard Model (SM). However, it cannot explain some deviations from the SM, such as the baryon asymmetry in the Universe [3]. Possible solutions can be derived from two Higgs doublet models (2MDMs), which are simple and natural extensions to the Standard Model. They provide possible explanations for why the top quark is so much heavier than other elementary fermions [4], why the up quark is so much lighter than charm and top quark [5], and provide additional sources of CP violation [6–8] to explain the observed baryon asymmetry of the Universe.

General 2HDMs lead to a rich phenomenology at the CERN Large Hadron Collider (LHC), including a Higgs pseudoscalar (A^0), a pair of charged Higgs bosons (H^\pm), and a heavier Higgs scalar (H^0). Furthermore, there could be significant flavor changing neutral currents mediated by the CP-even heavy scalar and the CP-odd pseudoscalar, as well as enhanced charged Higgs decay ($H^+ \rightarrow c\bar{b}$) without CKM (V_{cb}) suppression [9]. The SM expectation is $\mathcal{B}(t \rightarrow ch^0) \approx 10^{-14}$ [10–12], which is significantly less than current and near term experiments can observe. If this FCNH signal is observed at the LHC, it would imply physics beyond the Standard Model [13–29].

We adopt the Yukawa Lagrangian in a general two Higgs doublet model [30, 31] as

$$\begin{aligned} \mathcal{L}_Y = & \frac{-1}{\sqrt{2}} \sum_{F=U,D,L} \bar{F} \left\{ [\kappa^F s_{\beta-\alpha} + \rho^F c_{\beta-\alpha}] h^0 + [\kappa^F c_{\beta-\alpha} - \rho^F s_{\beta-\alpha}] H^0 \right. \\ & \left. - i \operatorname{sgn}(Q_F) \rho^F A^0 \right\} P_R F - \bar{U} [V \rho^D P_R - \rho^{U\dagger} V P_L] D H^+ - \bar{\nu} [\rho^L P_R] L H^+ + \text{H.c.} \end{aligned} \quad (1)$$

where $P_{L,R} \equiv (1 \mp \gamma_5)/2$, $c_{\beta-\alpha} \equiv \cos(\beta-\alpha)$, $s_{\beta-\alpha} \equiv \sin(\beta-\alpha)$, α is the mixing angle between neutral Higgs scalars, $\tan \beta \equiv v_2/v_1$ is the ratio of the vacuum expectation values of the two Higgs doublets [32], Q_F is the fermion charge, and the κ matrices are diagonal and fixed by fermion masses to $\kappa^F = \sqrt{2} m_F / v$ with $v \approx 246$ GeV, while the ρ matrices contain both diagonal and off-diagonal elements with free parameters. In addition, F, U, D, L represent the elementary fermions, up-type quarks, down-type quarks, and charged leptons, respectively. The matrix elements ρ are the FCNH couplings to the fermions. The consistency between experimental data and the Standard Model [33, 34], implies that all two Higgs doublet models must be in the alignment limit [35, 36] with one SM-like 125 GeV light scalar (h^0).

According to recent searches for $t \rightarrow ch^0$ with the Higgs boson decaying into final states with leptons as well as $h^0 \rightarrow b\bar{b}$ and $h^0 \rightarrow \gamma\gamma$, the ATLAS Collaboration [28], and the CMS Collaboration [29] placed a strong constraint on the branching fraction $\mathcal{B}(t \rightarrow ch^0) \leq 3.7 \times 10^{-4}$, which leads to an upper limit on the FCNH Yukawa coupling $|\lambda_{tch}|$

$$\lambda_{tch} \leq 0.036, \quad (2)$$

with the relation between λ_{tch} and the $t \rightarrow ch^0$ branching fraction [37] being

$$\lambda_{tch} \approx 1.92 \times \sqrt{\mathcal{B}(t \rightarrow ch^0)}, \quad (3)$$

$|\lambda_{tch}| = \tilde{\rho}_{tc} \cos(\beta - \alpha)$, and

$$\tilde{\rho}_{tc} \approx \sqrt{(|\rho_{tc}|^2 + |\rho_{ct}|^2)/2} \quad (4)$$

where the ρ matrix can be chosen to be non-Hermitian such that $|\rho_{ct}| < |\rho_{tc}|$. Therefore, the effective Lagrangian for H^0 and A^0 can be written as,

$$\mathcal{L} = \frac{\lambda_{tcH}}{\sqrt{2}} \bar{c}tH^0 + i \frac{\lambda_{tcA}}{\sqrt{2}} \bar{c}tA^0 + H.c. \quad (5)$$

where

$$|\lambda_{tcH}| = \tilde{\rho}_{tc} \sin(\beta - \alpha) \quad \text{and} \quad |\lambda_{tcA}| = \tilde{\rho}_{tc} \quad (6)$$

are not suppressed in the alignment limit.

In a previous study [38], we demonstrated that employing the collinear approximation [39–41] for $h^0 \rightarrow \tau\tau \rightarrow \ell^+\ell^- + \cancel{E}_T$, $\ell^\pm = e^\pm, \mu^\pm$, in charming top decays of $t \rightarrow ch^0$, we can reconstruct the Higgs and the top quark effectively at the LHC. In this article, we investigate the discovery potential of H^0 or A^0 through flavor changing top quark decays ($t \rightarrow c\phi^0$) followed by the Higgs boson decaying into $\tau^+\tau^-$ with one τ decaying leptonically and the other decaying hadronically ($\tau^+\tau^- \rightarrow \ell^\pm j_\tau + \cancel{E}_T$) at the LHC, where \cancel{E}_T is the missing transverse energy in the event from the neutrinos.

We perform a Monte Carlo simulation using MADGRAPH 5 [42], PYTHIA 8 [43] and DELPHES [44], and compare with a parton level analysis to study the FCNH decay of one top quark while the other top quark decays hadronically to a bottom quark (b) and two light jets: $pp \rightarrow t\bar{t} \rightarrow bW^\pm c\phi^0 \rightarrow bj j c\tau^+\tau^- + X$, where X represents the other particles produced in the pp collision. We have calculated the production rates using the full tree level matrix elements including the Breit-Wigner resonance for both the signal and the background processes.

Since we did not apply charm tagging, our analysis is suitable for a general search for $t \rightarrow qh^0$, $q = u, c$. Many previous studies have adopted the Cheng-Sher Ansatz [45] as the benchmark Yukawa coupling

$$\lambda_{tqh} = \frac{\sqrt{2m_t m_q}}{v} \quad (7)$$

where $q = u, c$ and $v \approx 246$ GeV is the Higgs vacuum expectation value. The FCNH coupling, as the geometric mean for top and charm quark masses, is

$$\lambda_{tch} = \frac{\sqrt{2m_t m_c}}{v} \approx 0.09, \quad (8)$$

which has been excluded by recent ATLAS and CMS measurements [28, 29]. For simplicity, we assume $\lambda_{tch} \gg \lambda_{tuh}$ and focus on the search for $t \rightarrow ch^0$.

There are several aspects to note in this analysis. To reconstruct the Higgs boson and the real top quark, the collinear approximation of tau decays [46, 47] is used. The collinear approximation for reconstructed tau decays are required to have a momentum fractions x_i ($0 < x_i < 1$), where $x_i = p(\tau_{\text{vis}_i})/p(\tau_{\text{reco}})$, $i = 1, 2$, with τ_{vis_i} representing the visible component of the tau decay, either a light-lepton or jet, and τ_{reco} the reconstructed tau lepton, more effectively reduced the physics background than the centrality requirement suggested in Refs. [20, 22]. Furthermore, the energy of the charm quark in the top quark rest frame provides good acceptance for the FCNH top quark signal while rejecting background [15, 48]. Promising results are presented for the LHC with $\sqrt{s} = 14$ TeV.

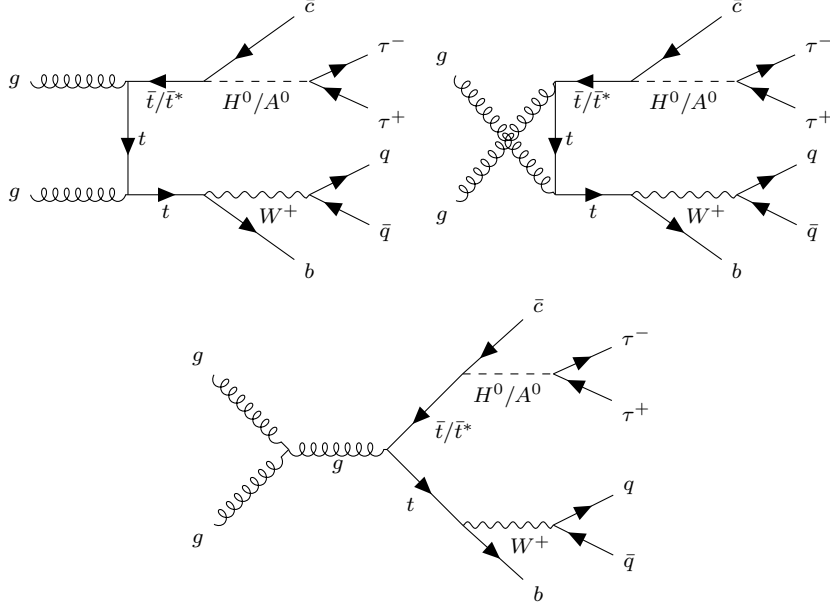


FIG. 1: Leading-order Feynman diagrams for the signal.

II. HIGGS SIGNAL AND EVENT SELECTIONS

This section presents the cross section and search strategy for the FCNH signal $pp \rightarrow t\bar{t} \rightarrow bj j \bar{c} \tau^+ \tau^- + X$ at the LHC. We focus on the discovery channel with one τ decaying hadronically ($\tau \rightarrow j_\tau \nu_\tau, j_\tau = \pi, \rho, \text{ or } a_1$), while the other tau lepton decays leptonically into a light-lepton (μ^\pm or e^\pm) and neutrinos. Therefore, the final state of our FCNH signal is $pp \rightarrow t\bar{t} \rightarrow (bj j)(\bar{c} \ell^\mp j_\tau) + \cancel{E}_T + X$. The leading-order Feynman diagrams are presented in Figure 1.

For our study, the matrix elements for $gg, q\bar{q} \rightarrow t\bar{t} \rightarrow bj j c \tau^+ \tau^-$ are generated using MADGRAPH 5 [42] at LO. In addition, we apply the collinear approximation for tau decays [46, 47], $\phi^0 \rightarrow \tau^+ \tau^- \rightarrow j_\tau \ell + \cancel{E}_T$. Since the Higgs boson is much more massive than the tau lepton ($m_\phi \gg m_\tau$), the taus from the Higgs decay are highly boosted. To a good approximation, the j_τ, ℓ^\pm , and neutrinos travel in the same direction as the tau lepton. Thus, we can reconstruct the Higgs boson mass from the invariant mass of the tau lepton pairs ($M_{\tau\tau}$).

The parton level cross section is evaluated using the CT14LO parton distribution functions (PDFs) [49]. For simplicity, the factorization scale (μ_F) and the renormalization scale (μ_R) are chosen to be the invariant mass of the top quark pair ($M_{t\bar{t}}$). With the above scale choices and PDFs, the K -factors are computed using TOP++ [50]. For all three LHC energies, $\sqrt{s} = 13, 13.6, \text{ and } 14$ TeV, the K -factors for top quark pair production are found to be approximately the same, around 1.8.

In the event level analysis, the parton level signal samples are generated using MADGRAPH [42, 51, 52] with 2HDM [53] model. Then the sample is processed by PYTHIA 8 [43], to simulate the parton showering and hadronization, and the τ decay by TAUOLA [54, 55]. Finally, detector simulation is applied to the events using DELPHES [44].

To provide a realistic estimate for production rates at the LHC, we evaluate the cross section for the FCNH signal and physics background in pp collisions with the proper tagging

and mistagging efficiencies. The ATLAS b -tagging efficiencies [56] are adopted to evaluate the cross section for the FCNH signal and physics background. The b -tagging efficiency is 0.7, the probability that a c -jet is mistagged as a b -jet (ε_c) is approximately 0.14, while the probability that a light jet (u, d, s, g) is mistagged as a b -jet (ε_j) is 0.01. For tau-jets (j_τ), we apply the ATLAS tagging efficiency $\varepsilon_\tau = 0.75$ (0.60) and mistagging efficiencies $\varepsilon_\tau(j) = 0.03$ (0.002) for 1-prong (3-prong) tau-jets, respectively, following Refs. [57, 58].

A. Event Selections

From the discussion of the signal in the previous section, every event is required to contain at least five jets, including exactly one identified b jet, one identified τ jet, and one light-lepton. We require events satisfy the following requirements, which are similar to the ATLAS and CMS $h^0 \rightarrow \tau^+\tau^-$ studies [59].

- (i) At least five jets with $p_T \geq 25$ GeV and $|\eta| \leq 2.5$. including one b -jet and one τ -jet,
- (ii) One lepton with $p_T \geq 20$ GeV and $|\eta| \leq 2.5$.
- (iii) An angular separation ($\Delta R = \sqrt{(\Delta\phi)^2 + (\Delta\eta)^2}$) greater than 0.4 is required between every pair of particles.
- (iv) Missing transverse energy $\cancel{E}_T \geq 30$ GeV.

Two light jets j_1 and j_2 , are selected by minimizing $|M_{jj} - m_W|$ and $|M_{bjj} - m_t|$. If the Higgs boson is lighter than the top quark ($m_\phi < m_t$), the c -jet is selected by minimizing $|M_{c\tau\tau} - m_t|$, where the τ leptons are reconstructed by applying the collinear approximation.

Since j_1 and j_2 result from W boson decay, their invariant mass distribution, $M_{j_1j_2}$, peaks at $m_W \approx 80.4$ GeV. Additionally, one top quark decays into a W boson and a b quark, thus $M_{bj_1j_2}$ has a peak at $m_t \approx 172.7$ GeV. Figures 2 and 3 present the invariant mass distribution of $M_{j_1j_2}$ and $M_{bj_1j_2}$, respectively, at both the parton and event level. Using the ATLAS mass resolution [60], we require the reconstructed W and top quark masses lie in the mass windows $\Delta M_{j_1j_2} = 0.20M_W$ and $\Delta M_{bj_1j_2} = 0.25m_t$.

B. Higgs Mass Reconstruction

For the FCNH signal, $t \rightarrow c\phi^0 \rightarrow c\tau^+\tau^- \rightarrow c\ell^\pm j_\tau + \cancel{E}_T$, we consider two situation: (a) for $m_\phi < 150$ GeV, the invariant mass $M_{\tau^+\tau^-}$ from the Higgs decay and the invariant mass of $c\tau^+\tau^-$ from the top quark decay are used, which produce peaks near m_ϕ and m_t , and (b) for $m_\phi > 150$ GeV, we only apply the $M_{\tau^+\tau^-}$ invariant mass reconstruction.

Figure 4 presents the invariant mass distributions $d\sigma/dM_{\tau\tau}$ for $m_H = 130$ GeV, 150 GeV, and 200 GeV. There are pronounced peaks near the Higgs boson mass for all values of the Higgs boson mass. The cross sections are evaluated for H^0 with $\tilde{\rho}_{tc} = 0.1$. In the alignment limit, the cross section of A^0 is comparable to that of H^0 . In addition, we present the invariant mass distributions $d\sigma/dM_{c\tau\tau}$ in Fig. 5 for $m_\phi = 130$ GeV and 150 GeV. There are pronounced peaks near the Higgs boson mass for $m_\phi \leq 150$ GeV. However, the peak of $M_{c\tau\tau}$ becomes very broad for $m_\phi > 150$ GeV. We require the reconstructed Higgs boson mass and top quark mass to lie in the mass windows (a) $\Delta M_{\tau\tau} = |M_{\tau\tau} - m_\phi| = 0.20m_\phi$ and (b) $\Delta M_{c\tau\tau} = |M_{c\tau\tau} - m_t| = 0.25m_t$ for $m_\phi < m_t - m_c$, using the ATLAS mass resolution [59].

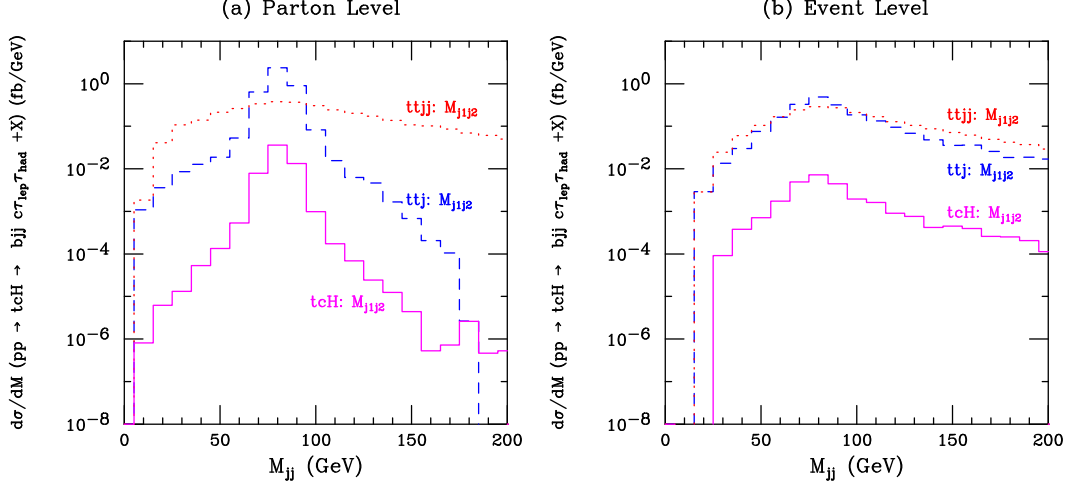


FIG. 2: Invariant mass distribution $d\sigma/dM_{jj}$ for the Higgs signal (magenta, solid) and for the dominant background from ttj (blue, dashed) and $ttjj$ (red, dotted) at the LHC with $\sqrt{s} = 13$ TeV. Results are shown for (a) parton level, and (b) event level.

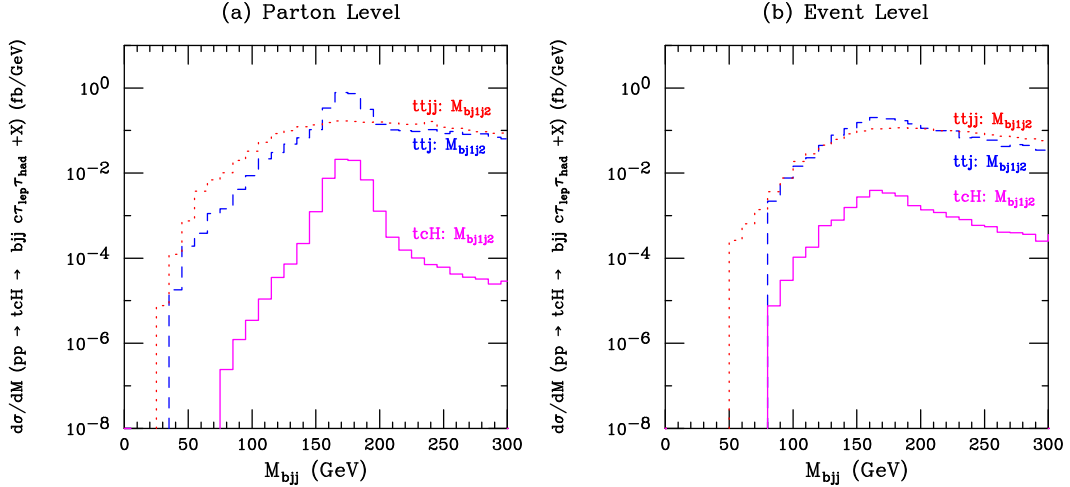


FIG. 3: Invariant mass distribution $d\sigma/dM_{bjj}$ for the Higgs signal (magenta, solid) and for the dominant background from ttj (blue, dashed) and $ttjj$ (red, dotted) at the LHC with $\sqrt{s} = 13$ TeV. Results are shown for (a) parton level, and (b) event level.

III. THE PHYSICS BACKGROUND

The dominant background to the signal is $t\bar{t}j$ ($j = q$ or g), with one top quark decaying leptonically ($t \rightarrow b\ell\nu$) the other decaying hadronically ($t \rightarrow bj\bar{j}$). The second most dominant background (about one third of the $t\bar{t}j$ background) is $t\bar{t}j(+\tau)$, $j = q$ or g with one top quark decaying leptonically ($t \rightarrow b\ell\nu$) and the other decaying into τ_{had} ($t \rightarrow b\tau_{had}\nu_\tau$). These two backgrounds contribute more than 95% of the total background.

In addition to all of the kinematic requirements and the invariant masses, the energy of the charm quark (E_c^*) in the rest frame of the top quark can be reconstructed to discriminate the $t \rightarrow c\phi^0$ signal from the background [15, 48]. For $m_\phi < m_t$, we can calculate the E_c^*

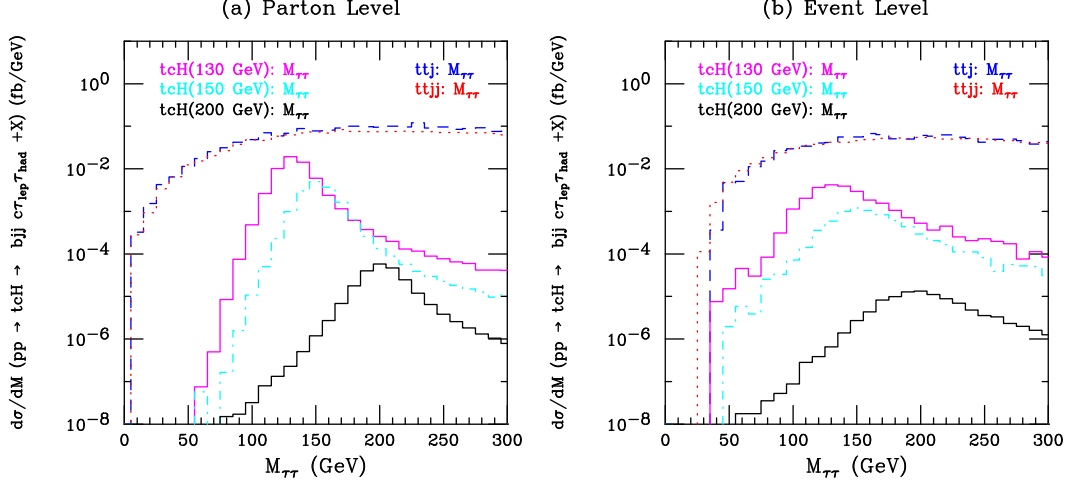


FIG. 4: Invariant mass distributions $d\sigma/dM_{\tau\tau}$ for the Higgs signal with $m_H = 130$ GeV (magenta, solid), 150 GeV (cyan, dot-dashed), 200 GeV (black, solid) and for the dominant background from ttj (blue, dashed) and $ttjj$ (red, dotted) at $\sqrt{s} = 13$ TeV. Results are shown for (a) parton level, and (b) event level with detector simulation in pp collisions.

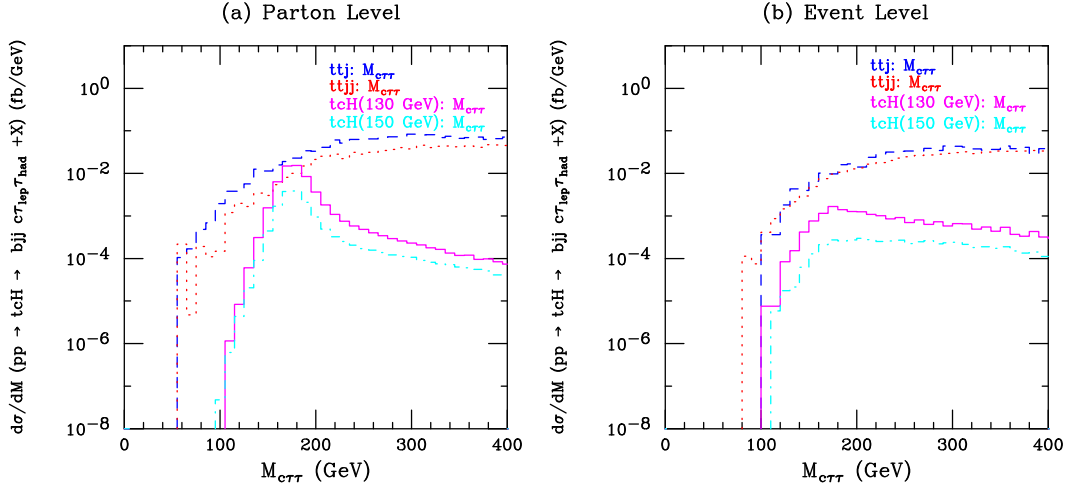


FIG. 5: Invariant mass distributions $d\sigma/dM_{c\tau\tau}$ for the Higgs signal ($t \rightarrow c\phi^0$) with $m_H = 130$ GeV (magenta, solid) and 150 GeV (cyan, dot-dashed) and for the dominant background from ttj (blue, dashed) and $ttjj$ (red, dotted) at $\sqrt{s} = 13$ TeV. Results are shown for (a) parton level, and (b) event level with detector simulation in pp collisions.

from the following equation:

$$E_c^* = \frac{m_t}{2} \left[1 + \frac{m_c^2}{m_t^2} - \frac{m_\phi^2}{m_t^2} \right]. \quad (9)$$

Figure 6 presents the energy distributions of the charm quark in the top quark rest frame for the two main backgrounds and for $m_\phi = 130$ GeV and 150 GeV, which exhibit enhancements at 37.4 GeV and 21.2 GeV, respectively. Selecting events with $E_c^* < 60$ GeV removes a larger fraction of background events than signal events, thereby enhancing the discovery potential.

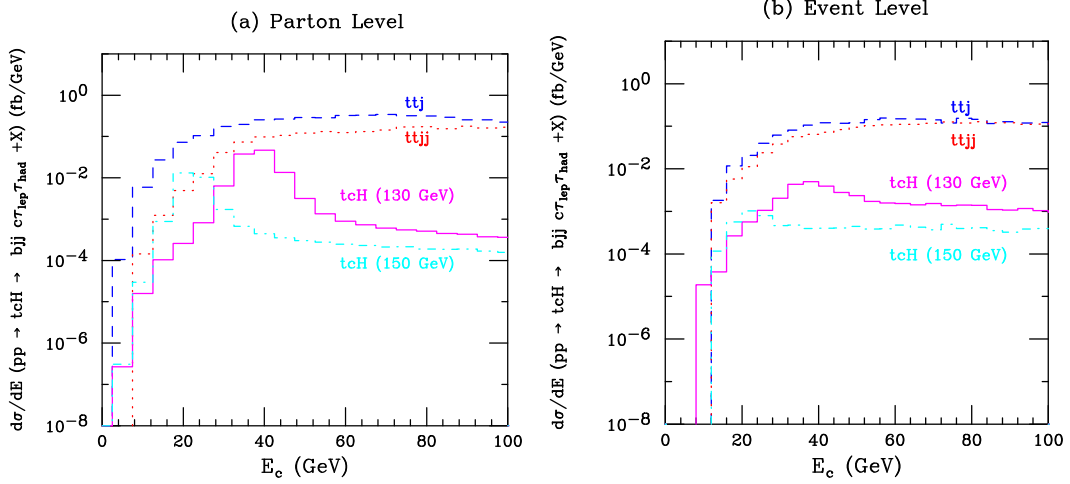


FIG. 6: Energy distribution for the charm quark ($d\sigma/dE_c$) in the top quark rest frame for the Higgs signal from $t \rightarrow cH^0$ with $m_H = 130$ GeV (magenta, solid), 150 GeV (cyan, dot-dashed) and for the dominant background from ttj (blue, dashed) and $ttjj$ (red, dotted) at $\sqrt{s} = 13$ TeV. Results are shown for (a) parton level, and (b) event level with detector simulation in pp collisions.

From the invariant mass and the charm quark energy distributions at the parton and event levels, the following mass requirements are deduced

- (i) $|M_{j_1j_2} - m_W| \leq 0.20 \times m_W$ and $|M_{bj_1j_2} - m_t| \leq 0.25 \times m_t$,
- (ii) $|M_{\tau\tau} - m_\phi| \leq 0.20 \times m_\phi$,
- (iii) $|M_{c\tau\tau} - m_t| \leq 0.25 \times m_t$ for $m_\phi \leq 150$ GeV,
- (iv) $0 \text{ GeV} \leq E_c^* \leq 60 \text{ GeV}$ for $m_\phi \leq 150$ GeV.

For the case $m_\phi > 150$ GeV, we only apply (i) and (ii) to the signal and background events. These requirements are chosen to reduce the physics background in a manner that maximizes the statistical significance of the signal.

IV. DISCOVERY POTENTIAL AT THE PARTON LEVEL AND EVENT LEVEL

We present the parton level signal cross sections at $\sqrt{s} = 13, 13.6, \text{ and } 14$ TeV, after applying all the selection criteria (see Table I) for $\tilde{\rho}_{tc} = 0.1$ and 0.5, in Table II. The cross sections for the backgrounds after applying the selection requirements are presented in Table III.

Applying all the selection requirements, we present the signal cross sections at the event level in Table IV for $m_H = 130$ GeV, 150 GeV, and 200 GeV as well as $\tilde{\rho}_{tc} = 0.1$ and 0.5. The event level cross sections for the dominant physics backgrounds are shown in Table V. We evaluate the statistical significance (N_{SS}) as a function of $\tilde{\rho}_{tc}$ and m_ϕ from this study, where N_{SS} is calculated using [61]

$$N_{SS} = \sqrt{2(N_S + N_B) \ln(1 + N_S/N_B) - 2N_S}. \quad (10)$$

Selection Criteria	S ₁	BG ₁	S ₂	BG ₂
≥ 5 jets, 1 lepton	✓	✓	✓	✓
1 tagged b -jet, 1 tagged τ -jet	✓	✓	✓	✓
$p_T(b, j) > 25$ GeV, $ \eta(j) < 2.5$	✓	✓	✓	✓
$p_T(l) > 20$ GeV, $ \eta(l) < 2.5$	✓	✓	✓	✓
$\Delta R > 0.4$	✓	✓	✓	✓
$\cancel{E}_T > 30$ GeV	✓	✓	✓	✓
$ M_{j_1 j_2} - m_W \leq 0.20 \times m_W$	✓	✓	✓	✓
$ M_{b j_1 j_2} - m_t \leq 0.25 \times m_t$	✓	✓	✓	✓
$ M_{\tau\tau} - m_\phi \leq 0.20 \times m_\phi$	✓	✓	✓	✓
$ M_{c\tau\tau} - m_t \leq 0.25 \times m_t$	✓	✓	–	–
$0 \text{ GeV} \leq E_c^* \leq 60 \text{ GeV}$	✓	✓	–	–

TABLE I: Selection criteria for signal and backgrounds events for $m_\phi \leq 150$ GeV and $m_\phi > 150$ GeV. In this table, S₁ represents signal events with $m_\phi \leq 150$ GeV and BG₁ its background, S₂ represents signal events with $m_\phi > 150$ GeV and BG₂ its background.

$\sqrt{s} = 13$ TeV	$\rho_{tc} = 0.1$	$\rho_{tc} = 0.5$
$m_H = 130$ GeV	0.3857 fb	9.657 fb
$m_H = 150$ GeV	0.1166 fb	2.889 fb
$m_H = 200$ GeV	0.0016 fb	0.0023 fb
$\sqrt{s} = 13.6$ TeV	$\rho_{tc} = 0.1$	$\rho_{tc} = 0.5$
$m_H = 130$ GeV	0.4241 fb	10.58 fb
$m_H = 150$ GeV	0.1300 fb	3.231 fb
$m_H = 200$ GeV	0.0018 fb	0.0025 fb
$\sqrt{s} = 14$ TeV	$\rho_{tc} = 0.1$	$\rho_{tc} = 0.5$
$m_H = 130$ GeV	0.4567 fb	11.47 fb
$m_H = 150$ GeV	0.1370 fb	3.434 fb
$m_H = 200$ GeV	0.0020 fb	0.0027 fb

TABLE II: Parton level signal cross sections after all selection criteria are applied and b -jet and tau-jet efficiencies $\varepsilon_b = 0.7$ and $\varepsilon_\tau = 0.723$, respectively.

Here N_S and N_B are number of signal and background events, where $N_S = \sigma_s \times L$, $N_B = \sigma_b \times L$, and L is the integrated luminosity of the LHC.

Figure 7 presents the signal cross section as a function of the heavy Higgs boson mass for $\tilde{\rho}_{tc} = 0.1$ and 0.5. In the alignment limit of 2HDM with $\sin(\beta - \alpha) \rightarrow 1$, the cross section for H^0 production is comparable to that of the A^0 . For the case that $m_H \simeq m_A$, the signal cross section and the statistical significance is doubled. We observe that the cross section declines rapidly as m_H increases for $m_H < m_t$ and m_H is closer to m_t as the charm quark becomes less energetic, but decreases slowly for $m_H > m_t$. This indicates that the impact of m_H becomes less significant when t or \bar{t} become virtual and $H^0 \rightarrow t\bar{c}$ decay channel opens up. Figure 8 presents the signal cross section as a function of $\tilde{\rho}_{tc}$ for $m_H = 130, 150,$ and 200 GeV. For $m_H < m_t$, the cross section increases approximately as $\sqrt{\tilde{\rho}_{tc}}$. However, for $m_H > m_t$, the

$\sqrt{s} = 13$ TeV	$t\bar{t}j$	$t\bar{t}jj(+\tau)$	$Zb\bar{b}jj$	Total
$m_H = 130$ GeV	0.7236 fb	0.1458 fb	5.4×10^{-2} fb	0.8753 fb
$m_H = 150$ GeV	4.826 fb	1.144 fb	3.6×10^{-2} fb	6.005 fb
$m_H = 200$ GeV	8.145 fb	1.668 fb	1.2×10^{-2} fb	9.824 fb
$\sqrt{s} = 13.6$ TeV	$t\bar{t}j$	$t\bar{t}jj(+\tau)$	$Zb\bar{b}jj$	Total
$m_H = 130$ GeV	0.8010 fb	0.1568 fb	5.9×10^{-2} fb	0.9640 fb
$m_H = 150$ GeV	5.326 fb	1.281 fb	4.0×10^{-2} fb	6.647 fb
$m_H = 200$ GeV	9.052 fb	1.849 fb	1.1×10^{-2} fb	10.91 fb
$\sqrt{s} = 14$ TeV	$t\bar{t}j$	$t\bar{t}jj(+\tau)$	$Zb\bar{b}jj$	Total
$m_H = 130$ GeV	0.8586 fb	0.1667 fb	6.3×10^{-2} fb	1.031 fb
$m_H = 150$ GeV	5.683 fb	1.378 fb	4.3×10^{-2} fb	7.103 fb
$m_H = 200$ GeV	9.639 fb	1.978 fb	1.2×10^{-2} fb	11.63 fb

TABLE III: Background cross sections after applying the mass selection at the parton level.

$\sqrt{s} = 13$ TeV	$\rho_{tc} = 0.1$	$\rho_{tc} = 0.5$
$m_H = 130$ GeV	0.1589 fb	3.474 fb
$m_H = 150$ GeV	0.0907 fb	2.317 fb
$m_H = 200$ GeV	1.1×10^{-3} fb	1.5×10^{-3} fb
$\sqrt{s} = 13.6$ TeV	$\rho_{tc} = 0.1$	$\rho_{tc} = 0.5$
$m_H = 130$ GeV	0.1685 fb	4.108 fb
$m_H = 150$ GeV	0.1026 fb	2.677 fb
$m_H = 200$ GeV	1.2×10^{-3} fb	1.8×10^{-3} fb
$\sqrt{s} = 14$ TeV	$\rho_{tc} = 0.1$	$\rho_{tc} = 0.5$
$m_H = 130$ GeV	0.1894 fb	8.050 fb
$m_H = 150$ GeV	0.1031 fb	5.638 fb
$m_H = 200$ GeV	1.4×10^{-3} fb	2.0×10^{-3} fb

TABLE IV: Event level signal cross sections after all selections are applied.

cross section is approximately constant. This indicates for $m_H > m_t$ the $H^0 \rightarrow t\bar{c}$ decay channel suppresses the $H^0 \rightarrow \tau^+\tau^-$ branching fraction. That means the enhancement from $\tilde{\rho}_{tc}^2$ in the production of $pp \rightarrow t\bar{t} \rightarrow tc\phi^0 \rightarrow tc\tau^+\tau^- + X$ is almost cancelled by the total width when $H^0 \rightarrow t\bar{c}$ becomes the dominant decay channel for $\tilde{\rho}_{tc} \gtrsim 0.1$. Using 2HDMC [62], we calculate and present the branching fractions of the relevant Higgs decay channels in Fig. 9.

Figure 10 presents the 5σ discovery significance at the LHC for $\sqrt{s} = 13.6$ TeV and Fig. 11 presents the discovery contours for $\sqrt{s} = 14$ TeV. The discovery potential are shown for both parton level and event level in the $[m_\phi, \tilde{\rho}_{tc}]$ plane. We have chosen three values of the integrated luminosity $\mathcal{L} = 30, 300$ and 3000 fb^{-1} . It is clear for masses of Higgs boson less than the mass of top quark, the high luminosity LHC at $\sqrt{s} = 14$ TeV with an integrated luminosity $L = 3000 \text{ fb}^{-1}$ significantly improves the discovery potential for the FCNH signal.

$\sqrt{s} = 13 \text{ TeV}$	$t\bar{t}j$	$t\bar{t}jj(+\tau)$	$Zb\bar{b}jj$	Total
$m_H = 130 \text{ GeV}$	0.7157 fb	0.3559 fb	$1.6 \times 10^{-2} \text{ fb}$	1.088 fb
$m_H = 150 \text{ GeV}$	4.689 fb	1.904 fb	$4.1 \times 10^{-2} \text{ fb}$	6.635 fb
$m_H = 200 \text{ GeV}$	6.860 fb	2.720 fb	$1.4 \times 10^{-2} \text{ fb}$	9.594 fb
$\sqrt{s} = 13.6 \text{ TeV}$	$t\bar{t}j$	$t\bar{t}jj(+\tau)$	$Zb\bar{b}jj$	Total
$m_H = 130 \text{ GeV}$	0.8734 fb	0.3982 fb	$2.5 \times 10^{-2} \text{ fb}$	1.297 fb
$m_H = 150 \text{ GeV}$	5.098 fb	2.173 fb	$4.3 \times 10^{-2} \text{ fb}$	7.313 fb
$m_H = 200 \text{ GeV}$	7.065 fb	3.200 fb	$2.2 \times 10^{-2} \text{ fb}$	10.29 fb
$\sqrt{s} = 14 \text{ TeV}$	$t\bar{t}j$	$t\bar{t}jj(+\tau)$	$Zb\bar{b}jj$	Total
$m_H = 130 \text{ GeV}$	0.9331 fb	0.4034 fb	$2.7 \times 10^{-2} \text{ fb}$	1.364 fb
$m_H = 150 \text{ GeV}$	5.544 fb	2.266 fb	$5.0 \times 10^{-2} \text{ fb}$	7.859 fb
$m_H = 200 \text{ GeV}$	7.367 fb	3.204 fb	$2.9 \times 10^{-2} \text{ fb}$	10.60 fb

TABLE V: Background cross sections after applying the mass selection at the event level.

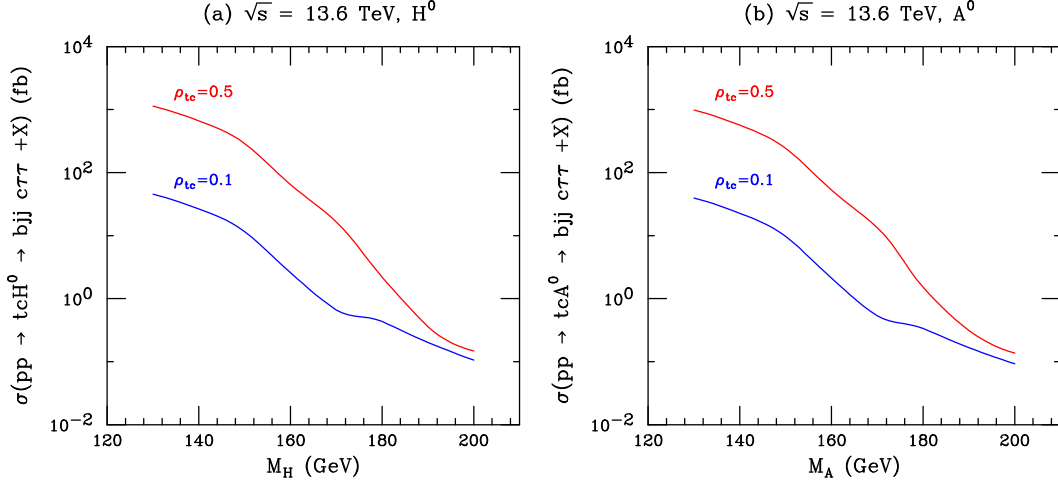


FIG. 7: Signal cross section σ vs. mass of Higgs boson for the FCNH signal ($t \rightarrow c\Phi^0$) with $\rho_{tc} = 0.1$ (blue) and 0.5 (red) at $\sqrt{s} = 13.6 \text{ TeV}$, where ϕ^0 is (a) Heavy Scalar H^0 , and (b) pseudoscalar A^0 with detector simulation in pp collisions.

V. CONCLUSIONS

In a general 2HDM [30, 31], flavor-changing interactions involving the neutral heavy Higgs bosons (H^0 and A^0) are not suppressed in the alignment limit [35, 36]. In this limit, characterized by $\cos(\beta - \alpha) \approx 0$, the light Higgs boson (h^0) mimics the Standard Model Higgs boson, h_{SM}^0 . As a result, searches for $t \rightarrow ch^0$ and $t \rightarrow cH^0$ are complementary, given that the relevant flavor-changing couplings are $\lambda_{tch} = \rho_{tc} \cos(\beta - \alpha)$, $\lambda_{tch} = \rho_{tc} \sin(\beta - \alpha)$, and $\lambda_{tcA} = \rho_{tc}$. In particular, the decays $t \rightarrow cH^0$ and $t \rightarrow cA^0$ are directly sensitive to the FCNH coupling ρ_{tc} in the alignment limit with $\sin(\beta - \alpha) \approx 1$.

We investigated the discovery potential for such processes with a focus on $pp \rightarrow t\bar{t} \rightarrow tc\phi^0 + X$, $\phi^0 = H^0$ or A^0 where one top quark decays hadronically and the other through $t \rightarrow c\phi^0$ with subsequent $\phi^0 \rightarrow \tau^+\tau^- \rightarrow \tau_{lep}\tau_{had}$ decays at the LHC. One of the top quarks

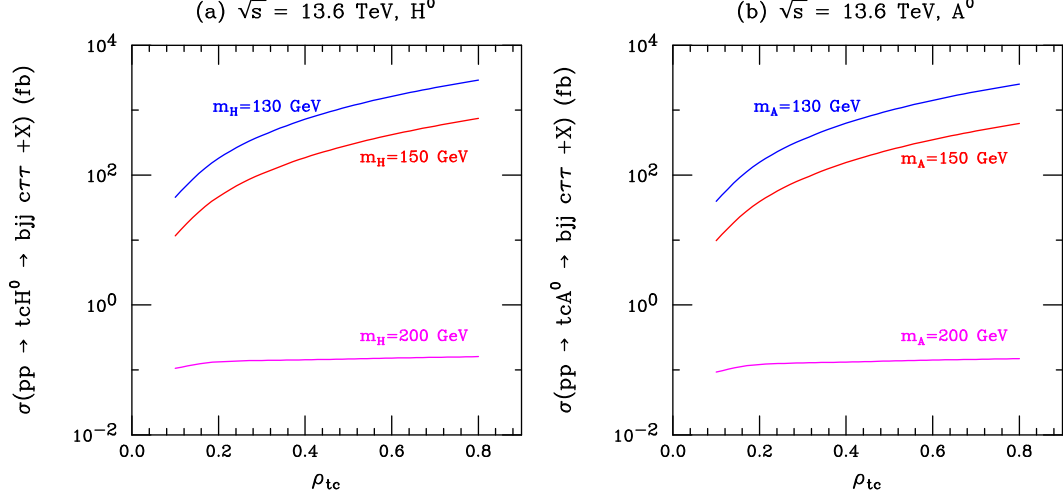


FIG. 8: Signal cross section σ vs. ρ_{tc} of Higgs boson for the FCNH signal ($t \rightarrow c\Phi^0$) with $m_\phi = 130$ GeV (blue), 150 GeV (red) and 200 GeV (magenta) at $\sqrt{s} = 13.6$ TeV, where Φ^0 is (a) Heavy Scalar H^0 , and (b) pseudoscalar A^0 with detector simulation in pp collisions.

can become virtual if $m_H > m_t$. The two primary physics backgrounds to this signal are (a) $t\bar{t}j$ with one top quark decaying hadronically and the other decaying leptonically, and (b) $t\bar{t}jj$ with both top quarks decaying leptonically. These can be reduced through the use of the following:

- (i) τ -tagging,
- (ii) collinear approximation to reconstruct τ decays,
- (iii) invariant mass of tau pairs peaking near the Higgs boson mass ($M_{\tau\tau} \approx m_\phi$),
- (iv) for $m_\phi < m_t$, the reconstructed top quark mass ($M_{c\tau\tau} \approx m_t$), and
- (v) for $m_\phi < m_t$, the charm quark energy $E_c \approx E_c^*$ in the top quark rest frame.

Based on our event level analysis, we find that the LHC at $\sqrt{s} = 14$ TeV, with $\mathcal{L} = 3000 \text{ fb}^{-1}$, will be able to detect this FCNH signal for $\tilde{\rho}_{tc} \gtrsim 0.1$ and $m_\phi < 170$ GeV. In the case of degeneracy, $m_H \simeq m_A$, the signal cross section and the discovery significance can be doubled.

Acknowledgments

This research was supported in part by the U.S. Department of Energy and the University of Oklahoma.

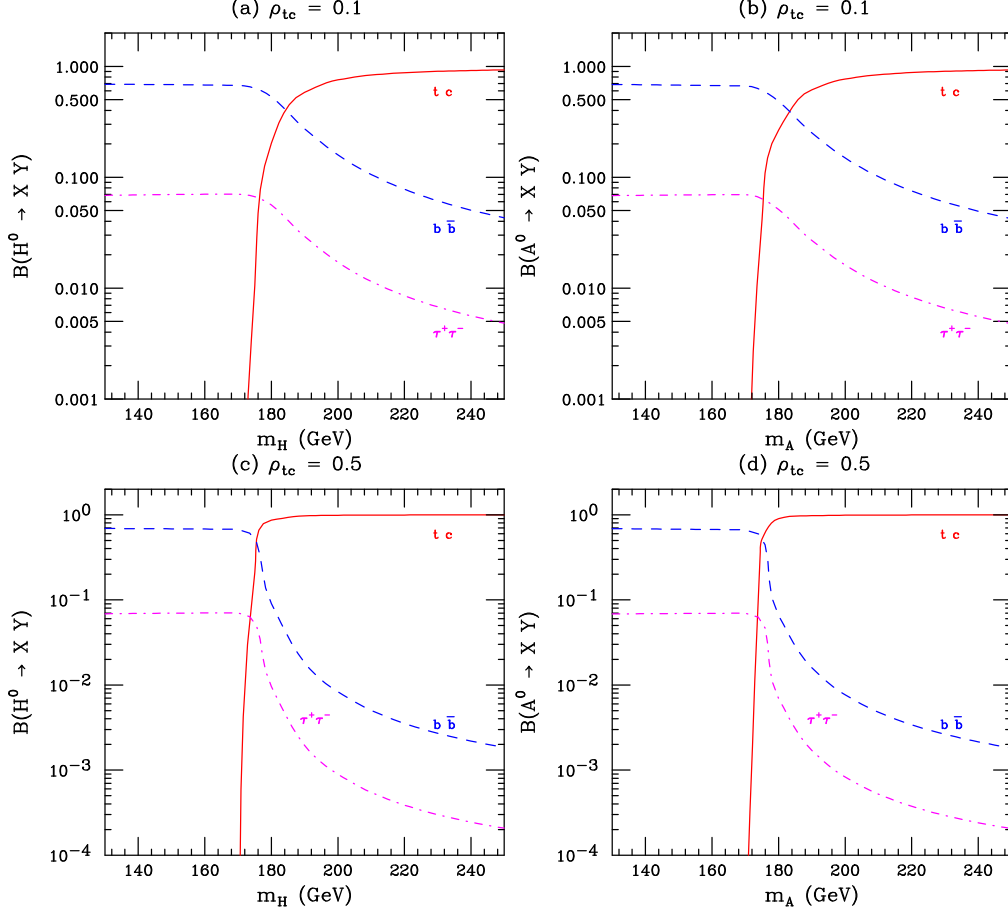


FIG. 9: Branching ratios of ϕ^0 as functions of m_ϕ for the following cases: (a) H^0 with $\tilde{\rho}_{tc} = 0.1$, (b) A^0 with $\tilde{\rho}_{tc} = 0.1$, (c) H^0 with $\tilde{\rho}_{tc} = 0.5$, and (d) A^0 with $\tilde{\rho}_{tc} = 0.5$.

-
- [1] G. Aad *et al.* [ATLAS], Phys. Lett. B **716**, 1-29 (2012).
 - [2] S. Chatrchyan *et al.* [CMS], Phys. Lett. B **716**, 30-61 (2012).
 - [3] A. D. Sakharov, Sov. Phys. Usp. **34**, no.5, 392-393 (1991).
 - [4] A. K. Das and C. Kao, Phys. Lett. B **372**, 106-112 (1996).
 - [5] Xu, Rui-Ming reportNumber = "UTTG-11-91", Phys. Rev. D **44** 590-592 (1991).
 - [6] Liu, Jiang and Wolfenstein, Lincoln, Nucl. Phys. B **289**, 1 (1987).
 - [7] S. Weinberg, Phys. Rev. D **42**, 860-866 (1990).
 - [8] K. Fuyuto, W. S. Hou and E. Senaha, Phys. Lett. B **776**, 402-406 (2018).
 - [9] D. K. Ghosh, W. S. Hou and T. Modak, Phys. Rev. Lett. **125**, no.22, 221801 (2020).
 - [10] J. A. Aguilar-Saavedra, Acta Phys. Polon. B **35**, 2695-2710 (2004).
 - [11] B. Mele, S. Petrarca and A. Soddu, Phys. Lett. B **435**, 401-406 (1998).
 - [12] G. Eilam, J. L. Hewett and A. Soni, Phys. Rev. D **44**, 1473-1484 (1991) [erratum: Phys. Rev. D **59**, 039901 (1999)].
 - [13] W. S. Hou, Phys. Lett. B **296**, 179-184 (1992).
 - [14] J. A. Aguilar-Saavedra and G. C. Branco, Phys. Lett. B **495**, 347-356 (2000).

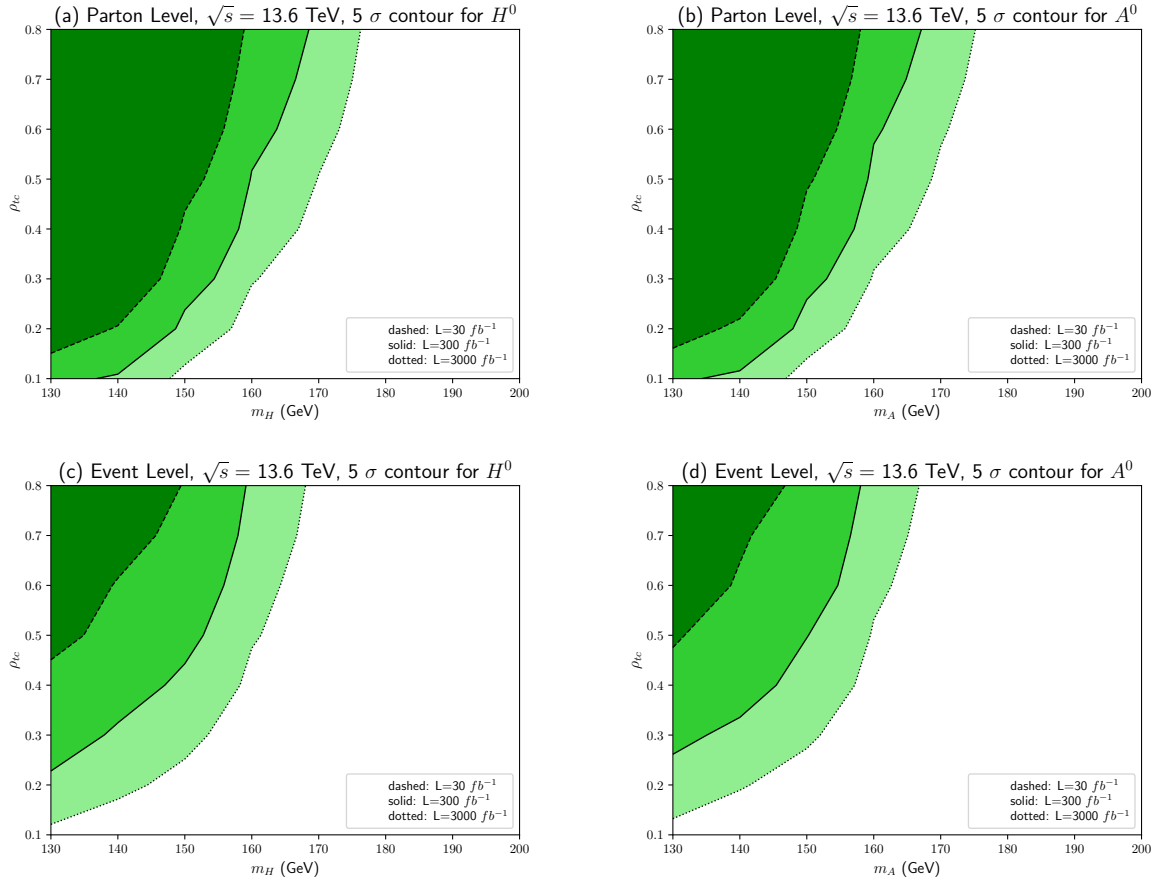


FIG. 10: Parton Level and Event Level 5σ discovery contours at the LHC at $\sqrt{s} = 13.6$ TeV in the $[m_\Phi, \tilde{\rho}_{tc}]$ plane for (a) Parton Level Heavy Scalar H^0 , (b) Parton Level pseudoscalar A^0 , (c) Event Level Heavy Scalar H^0 and (d) Event Level pseudoscalar A^0 with $L = 30fb^{-1}$ (dark green dotted dashed), $300fb^{-1}$ (medium green solid) and $L = 3000fb^{-1}$ (light green dashed)

- [15] C. Kao, H. Y. Cheng, W. S. Hou and J. Sayre, Phys. Lett. B **716**, 225-230 (2012).
- [16] K. F. Chen, W. S. Hou, C. Kao and M. Kohda, Phys. Lett. B **725**, 378-381 (2013).
- [17] D. Atwood, S. K. Gupta and A. Soni, JHEP **10**, 057 (2014).
- [18] V. Khachatryan *et al.* [CMS], Phys. Rev. D **90**, 112013 (2014).
- [19] G. Durieux, F. Maltoni and C. Zhang, Phys. Rev. D **91**, no.7, 074017 (2015).
- [20] X. Chen and L. Xia, Phys. Rev. D **93**, no.11, 113010 (2016).
- [21] V. Khachatryan *et al.* [CMS], JHEP **02**, 079 (2017).
- [22] M. Aaboud *et al.* [ATLAS], JHEP **05**, 123 (2019).
- [23] A. Papaefstathiou and G. Tetlalmatzi-Xolocotzi, Eur. Phys. J. C **78**, no.3, 214 (2018).
- [24] R. Jain and C. Kao, Phys. Rev. D **99**, no.5, 055036 (2019).
- [25] M. A. Arroyo-Ureña, R. Gaitán-Lozano, E. A. Herrera-Chacón, J. H. Montes de Oca Y. and T. A. Valencia-Pérez, JHEP **07**, 041 (2019).
- [26] N. Castro, M. Chala, A. Peixoto and M. Ramos, JHEP **10**, 038 (2020).
- [27] Y. J. Zhang and J. F. Shen, Eur. Phys. J. C **80**, no.9, 811 (2020).
- [28] G. Aad *et al.* [ATLAS], Eur. Phys. J. C **84**, no.7, 757 (2024).
- [29] A. Hayrapetyan *et al.* [CMS], Phys. Rev. D **112**, no.3, 032008 (2025).

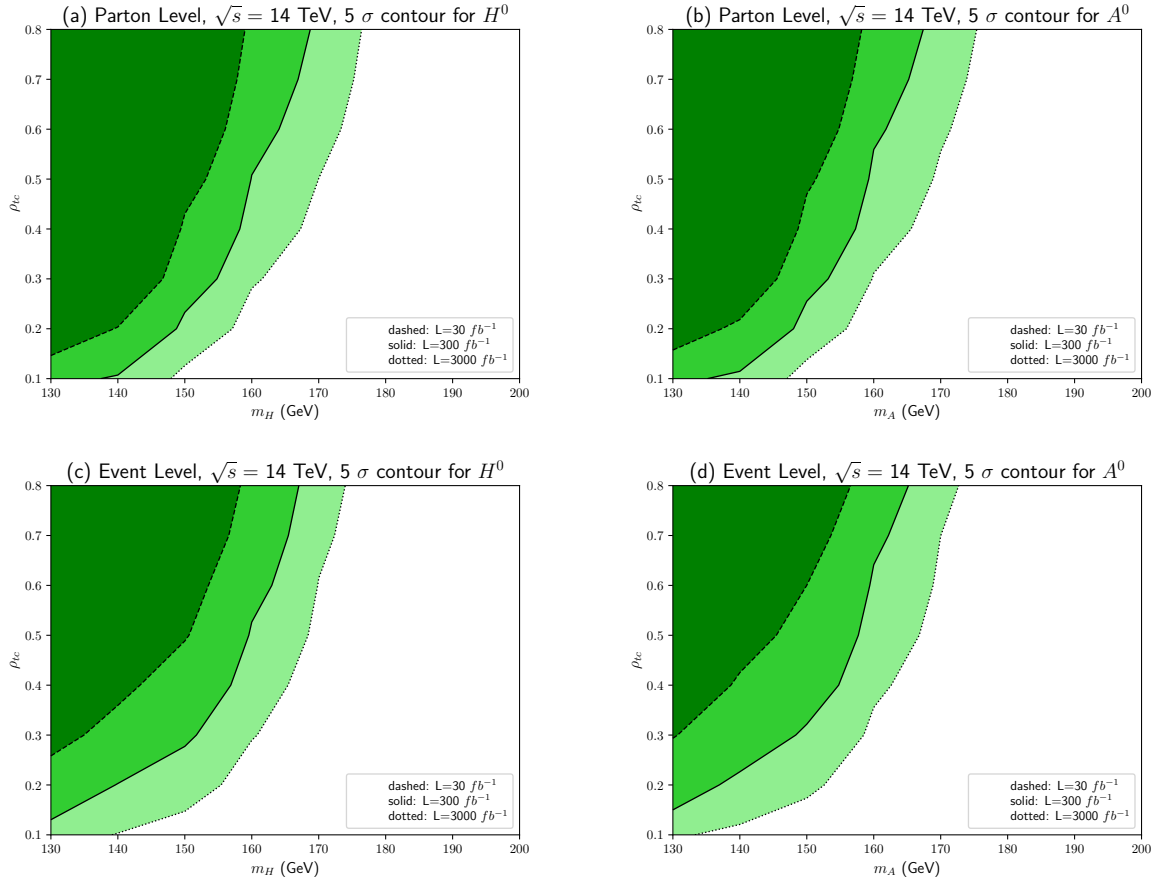


FIG. 11: Parton Level and Event Level 5σ discovery contours at the LHC at $\sqrt{s} = 14$ TeV in the $[m_\Phi, \tilde{\rho}_{tc}]$ plane for (a) Parton Level Heavy Scalar H^0 , (b) Parton Level pseudoscalar A^0 , (c) Event Level Heavy Scalar H^0 and (d) Event Level pseudoscalar A^0 with $L = 30 fb^{-1}$ (dark green dotted), $300 fb^{-1}$ (medium green solid) and $L = 3000 fb^{-1}$ (light green dashed)

- [30] S. Davidson and H. E. Haber, Phys. Rev. D **72**, 035004 (2005) [erratum: Phys. Rev. D **72**, 099902 (2005)].
- [31] F. Mahmoudi and O. Stal, Phys. Rev. D **81**, 035016 (2010).
- [32] J. F. Gunion, H. E. Haber, G. L. Kane and S. Dawson, *The Higgs Hunter's Guide*, (Addison-Wesley, Redwood City, 1990) ISBN 978-0201509359.
- [33] A. M. Sirunyan *et al.* [CMS], Eur. Phys. J. C **79**, no.5, 421 (2019).
- [34] G. Aad *et al.* [ATLAS], Phys. Rev. D **101**, no.1, 012002 (2020).
- [35] N. Craig, J. Galloway and S. Thomas, [arXiv:1305.2424 [hep-ph]].
- [36] M. Carena, I. Low, N. R. Shah and C. E. M. Wagner, JHEP **04**, 015 (2014).
- [37] ATLAS Collaboration, ATL-PHYS-PUB-2013-012.
- [38] P. Gutierrez, R. Jain and C. Kao, Phys. Rev. D **103**, no.11, 115020 (2021).
- [39] R. K. Ellis, I. Hinchliffe, M. Soldate and J. J. van der Bij, Nucl. Phys. B **297**, 221-243 (1988).
- [40] D. L. Rainwater, D. Zeppenfeld and K. Hagiwara, Phys. Rev. D **59**, 014037 (1998).
- [41] T. Plehn, D. L. Rainwater and D. Zeppenfeld, Phys. Rev. D **61**, 093005 (2000).
- [42] J. Alwall, M. Herquet, F. Maltoni, O. Mattelaer and T. Stelzer, JHEP **06**, 128 (2011).
- [43] T. Sjöstrand, S. Ask, J. R. Christiansen, R. Corke, N. Desai, P. Ilten, S. Mrenna, S. Prestel,

- C. O. Rasmussen and P. Z. Skands, *Comput. Phys. Commun.* **191**, 159-177 (2015).
- [44] J. de Favereau *et al.* [DELPHES 3], *JHEP* **02**, 057 (2014).
- [45] T. P. Cheng and M. Sher, *Phys. Rev. D* **35**, 3484 (1987).
- [46] K. Hagiwara, A. D. Martin and D. Zeppenfeld, *Phys. Lett. B* **235**, 198-202 (1990).
- [47] K. Hagiwara, T. Li, K. Mawatari and J. Nakamura, *Eur. Phys. J. C* **73**, 2489 (2013).
- [48] T. Han, J. Jiang and M. Sher, *Phys. Lett. B* **516**, 337-344 (2001).
- [49] S. Dulat, T. J. Hou, J. Gao, M. Guzzi, J. Huston, P. Nadolsky, J. Pumplin, C. Schmidt, D. Stump and C. P. Yuan, *Phys. Rev. D* **93**, no.3, 033006 (2016).
- [50] M. Czakon and A. Mitov, *Comput. Phys. Commun.* **185**, 2930 (2014).
- [51] J. Alwall, R. Frederix, S. Frixione, V. Hirschi, F. Maltoni, O. Mattelaer, H. S. Shao, T. Stelzer, P. Torrielli and M. Zaro, *JHEP* **07**, 079 (2014).
- [52] R. Frederix, S. Frixione, V. Hirschi, D. Pagani, H. S. Shao and M. Zaro, *JHEP* **07**, 185 (2018) [erratum: *JHEP* **11**, 085 (2021)].
- [53] C. Degrande, *Comput. Phys. Commun.* **197**, 239-262 (2015).
- [54] S. Jadach, J. H. Kuhn and Z. Was, *Comput. Phys. Commun.* **64**, 275-299 (1990).
- [55] S. Jadach, Z. Was, R. Decker and J. H. Kuhn, *Comput. Phys. Commun.* **76**, 361-380 (1993).
- [56] G. Aad *et al.* [ATLAS], *Eur. Phys. J. C* **79**, no.11, 970 (2019).
- [57] [ATLAS], ATL-PHYS-PUB-2015-045.
- [58] [ATLAS], ATL-PHYS-PUB-2019-033.
- [59] M. Aaboud *et al.* [ATLAS], *Phys. Rev. D* **99**, 072001 (2019).
- [60] G. Aad *et al.* [ATLAS], *JHEP* **11**, 150 (2019).
- [61] G. Cowan, K. Cranmer, E. Gross and O. Vitells, *Eur. Phys. J. C* **71** (2011), 1554 [erratum: *Eur. Phys. J. C* **73** (2013), 2501].
- [62] D. Eriksson, J. Rathsman and O. Stal, *Comput. Phys. Commun.* **181** (2010), 189-205.